

# Recent results from computer simulations of membrane channels and pumps

---

**Baumgaertner, Artur; Žuvić-Butorac, Marta; Grudinin, Sergei**

*Source / Izvornik:* **Recent Research Developments in Biophysics, 2003, 1 - 29**

**Book chapter / Poglavlje u knjizi**

*Publication status / Verzija rada:* **Published version / Objavljena verzija rada (izdavačev PDF)**

*Permanent link / Trajna poveznica:* <https://urn.nsk.hr/urn:nbn:hr:184:862899>

*Rights / Prava:* [Attribution-NonCommercial-NoDerivatives 4.0 International/Imenovanje-Nekomercijalno-Bez prerada 4.0 međunarodna](#)

*Download date / Datum preuzimanja:* **2024-05-13**



*Repository / Repozitorij:*

[Repository of the University of Rijeka, Faculty of Medicine - FMRI Repository](#)



# Recent Results from Computer Simulations of Membrane Channels and Pumps

Artur Baumgaertner<sup>+</sup>, Marta Zuvic-Butorac\*, Sergei Grudinin<sup>+†</sup>

<sup>+</sup>*Institute of Solid State Physics*, <sup>†</sup>*Institute for Structural Biology (IBI-2), Forschungszentrum Jülich, Germany*,

<sup>\*</sup>*Department of Physics, Faculty of Medicine, University of Rijeka, Croatia*

The present review reports on recent progress in modeling and simulation of biological ion channels and proton pumps. In particular, we describe the current approaches and results concerning permeation and selectivity of ion channels. This is demonstrated mainly at the example of a potassium ion channel. In the case of proton pumping across lipid membranes we report on recent results from computer simulation of bacteriorhodopsin. The distribution of internal water and the structure and dynamics of hydrogen-bonded networks inside bacteriorhodopsin are discussed.

## I. INTRODUCTION

Plasma membrane is the place where cell meets the external world and the structure that has not only to make a borderline, but also to connect the cell properly to the environment. The vast variety of membrane functions (transport of matter and energy, signal processing and transduction, etc.) is provided by a relatively simple structure of lipid bilayer with incorporated (integral) and/or attached (peripheral) proteins. Although the static picture might seem quite simple, the complexity of the system is far more seen in its dynamics. The membrane processes are governed by the short and long-range interactions that take place at very different time scales, ranging from picoseconds to hours.

As the lipid bilayer is permeable only for small non-polar molecules and hence impermeable for ions, the structural entities providing ion transport are membrane proteins. Generally, there are two types of transmembrane ion transport; the one that takes place down the electrochemical gradient for the specific ion (passive transport) and the opposite, “uphill” transport, that calls for an energy input in order to overcome the energy barrier (active transport). Respective protein structures are accordingly classified to ion channels (provide passive flow of ions) and ion pumps (ensure active ion transport).

A lot of experimental effort has been put into resolving membrane-bound processes, from the structural as well as dynamical point of view, but traditionally with a relatively small input from the theoretical approaches. The primary functional structures responsible for completion of membrane processes are proteins, so they have always called for the central attention. As far as the molecular structure determination of membrane proteins is concerned, obtaining a crystallized functional form of the membrane protein is still a generally non-solved problem; up to now, only few structures have been resolved up

to the atomic details. Consequently, modelling and simulations of membrane processes has been long facing the problem of lack in structural data, not to mention the problem of computational limitations for such a complex systems. Although the complete structure of channel forming antibiotic gramicidin A has been known for a long time [1] and a lot of computational modelling has been done on the structure [2, 3], it appeared that its structural and permeation properties differ from those of the biological channels, so the physiological relevance of the results is questioned.

The advantage of the simulation over experimental techniques has been widely seen in the possibility to explore the dynamical aspects of the structure which cannot be addressed experimentally. Every computer simulation study is at the first step confronted with the decision on the most appropriate level of detail to include in the description of the system. Generally, the majority of the membrane protein simulations fall into two categories: molecular dynamic (MD) studies or atomistic simulations, in which all the atoms of the system are treated explicitly, and mean-field or coarse-grained simulations, which treat some parts of the system as a continuum. Since the latter are less time consuming, those methods allow much longer simulation times, but are at the same confronted to a non-trivial issue of decision on the best mean-field model to be used.

As the atomic resolution of biological ion transport proteins became available during the last decade and the computational facilities gained more power, the theoretical modelling and simulation approach has consequently shifted from simple “hole in the wall” models to realistic structures embedded in the proper environment. This is, by and large seen in a recent progress in the field after the successful determination of highly resolved bacterial potassium channel KcsA [4–8], accompanied by the computational simulation of the structure [9–14], that almost com-

pleted the detailed picture of structure-function relationship for the potassium ion transport process.

At present, the amenable combination of atomistic resolution structures with highly sophisticated computational methods is considered to be a leading way to better understanding of fundamental properties of basic cell membrane physiology. The doubts about physiological relevance of results obtained on bacterial membrane proteins to those in mammalian cells have been lifted at least in the case of KcsA, for which there is evidence supporting evolutionary conservation of the architecture as well as of transporting properties [15, 16].

In this review we present some recent results from computer simulated structures of membrane ion channels and pumps. Special attention will be brought to the specific points revealed by simulations on bacterial potassium channel and light driven proton pump bacteriorhodopsin, that weren't observed experimentally, thus giving new insights to the research field.

## II. MEMBRANE CHANNELS

The membrane lipid bilayer is highly impermeable to ions, since the energy barrier for transferring a hydrated ion to the low dielectric environment of acyl chain region is prohibitively large. Thus the structure of lipid bilayer provides the cell capability of maintaining the intracellular ionic concentrations very much different to the extracellular ones. In general, potassium has about 30-fold higher intracellular concentration than extracellular, while sodium, chlorine and calcium are more concentrated outside. The difference in ionic concentrations gives rise to the existence of electric potential difference across the membrane, the inside of the cell being polarized negatively with respect to the outside.

Nevertheless, every cell has to have a pathway for ionic flow through the membrane in order to maintain proper physiological functioning. The membrane resting potential, which is predominantly determined by  $K^+$  concentration difference, can easily be changed by allowing the  $Na^+$  ions flow inside; if the membrane is depolarized, the resting potential is effectively restored by letting the  $K^+$  flow out; subtle changes in  $Ca^{2+}$  intracellular concentration can lead to a number of processes affecting important cell functions, etc.

Ion channels are transmembrane protein structures [17, 18] which ensure the continuous transport

pathway for diffusive flow of ions accross the membrane. As the direction of the ion flow through the channel is down the electrochemical gradient for the ion, the process is often referred to as a passive transport. Since the net flow of electric charge gives rise to a rapid change in transmembrane potential, ion channels play a key role in generating and propagating action potentials in nervous system. Moreover, it is well established that ion channels play important role in pathophysiology of various diseases and thereby present the primary targets for pharmacological drug design.

In order to assure the precisely controlled transmembrane ionic flow, ion channels have to be i) highly selective towards specific ion type (or highly discriminative for one ion type over all the other ions present), and ii) have to have well defined gating control mechanism. The protein conformation of the open state, in which the selected ions are allowed to pass, has to be accomplished upon specific stimulus; the known mechanisms include change in transmembrane potential (voltage-gated ion channels), binding of another molecule (ligand-gated or receptor-gated channels) and mechanical stress (mechanosensitive channels or stretch-gated channels).

Although the experimentally determined rate of ion transport through different channels varies (according to the channel type, concentration difference and transmembrane potential) and ranges from  $10^6$  to  $10^9$  ions/s, the simple calculation in given circumstances reveals that this rapid transport is almost at the diffusion rate. This fact is indicating that an open channel structure is ensuring energetically almost barrierless pathway for selected ion flow. Additionally, the variability among channels is also seen in the geometry of ion-transport pathway, but there seem to be two characteristic regions appearing as a general feature of all biological channels: a wider cavity that accomodates hydrated ions and a short and narrow selectivity filter. Moreover, those two regions seem to be evolutionary conserved, at least in specific channel type (e.g. potassium channels) [15, 19].

Ion channels are functionally and structurally simplest among the membrane transport proteins, since the transport itself doesn't call for a (major) conformational changes of protein structure. Conformational changes occur in the process of gating, i.e. are needed for discrimination between opened (permeable to selected ions) and closed (impermeable to all ions present) channel states.

There are three major experimentally determined descriptors of channel function : 1) high selectivity

towards one ion specie 2) permeation process that ensures rapid transport at given rate, defining the conductance of the channel (I-V curves of the majority of biological channels are linear within the physiological range of membrane potentials), and 3) gating mechanism. Those descriptors are the very same that every theoretical modelling has to reproduce and give insight to understanding.

At present, no single computational technique can describe all the functional properties of an ion channel. The choice of the level for the theoretical approach and the use of the computational technique to describe processes of selectivity, permeation and gating of an ion channel, depend essentially on the timescale of the process itself. While the timescale of the permeation process for typical channel is in the order of few tenths of ns, the gating takes the time in the order of ms. At the present state of computational speed neither of the processes can be completed using MD techniques, but call for more coarse-grained modelling. On the other hand, since BD and continuum theories do not distinguish between monovalent ions, the modelling of channel selectivity can only be done using MD approach. Although Brownian dynamics (BD) simulations have provided usefull data on the total permeation process of ions through channels [20], their reliability concerning details is limited due to the coarse-graining of the channel structure and applications of mean-field approximations of water and lipids. More details, including fluctuations of all constituents of the channel and its environment (all atom model of channel, water and lipids) have been elucidated by use of molecular dynamics (MD) simulations [21, 22] albeit quite limited in time to the few nanoseconds time regime.

Nevertheless, every computational modelling of ion channels requires detailed knowledge on the structure. Although ion channels have been experimentally identified more than 25 years ago (thanks to the invention of patch-clamp technique, by Neher and Sackmann [23]), there are nowadays only few of the channel protein structures that are known up to atomic resolution details. The main obstacle in resolving those structures has been, as for all the membrane proteins, the experimental problem in obtaining crystallized functional form of the channel. Recent determination of highly resolved bacterial potassium channel [4–8] immediately raised very much attention in the field of computational modelling, so several groups have conducted molecular dynamics [9–13], Brownian dynamics simulations [24] and free energy perturbation studies [25, 26].

## A STRUCTURE

In order to support the reliability to the results of MD simulations of a full all-atom model of an ion channel (including the channel, the water and the lipid bilayer), it is important to carefully prepare the starting configuration. In particular, the embedding of the crystal structure into a pre-equilibrated membrane-water system is a non-trivial task, since the insertion of the structure into a prepared cavity in the membrane-water system leaves many local vacancies between the two systems. A too rapid subsequent equilibration renders the channel structure to unfold. The typical r.m.s. deviation between the original and this type of equilibrated structure can be of the order of few Å. Obviously, this type of modified structure may not provide correct insights into permeation and selectivity mechanism of the channel. Therefore a comparison between the crystal structure and the simulation-mediated equilibrated structure is important.

**The KcsA Potassium Channel.** It has been shown that the simulated KcsA channel structure [11, 13, 27] is still very similar to the original structure. The r.m.s. deviation of the  $C_\alpha$  atoms between the crystal structure and the simulated structure is about 3.7 Å [27], which is comparable to the crystal structure of 3.2 Å resolution [4]. Even the more recently KcsA structure at 2.0 Å resolution [6] has some specific similarities with the simulated structure [27], at least concerning the widening of the extracellular mouth, which is indicated by a careful analysis of the radii of gyration of the various residues of the KcsA channel. The radius of gyration  $R_g$  of each residue  $i$  is defined as follows:

$$R_g^{(i)} = \frac{1}{4} \sum_{\alpha=1}^4 \left[ \vec{r}_\alpha^{(i)} - \langle \vec{r}^{(i)} \rangle \right]^2 \quad (1)$$

where  $\langle \vec{r}^{(i)} \rangle = \frac{1}{4} \sum_{\alpha=1}^4 \vec{r}_\alpha^{(i)}$  and  $\vec{r}_\alpha^{(i)}$  is the center of mass of each residue in the  $\alpha$ th subunit of the tetramer, the index  $23 \leq i \leq 119$  labels the residues of the crystal structure [4], and  $\langle \dots \rangle$  denotes the ensemble averaging. All simulations indicate that the KcsA structure remains closed at the intracellular mouth. It should be noted that the fluctuation profile of the radius of gyration of each residue along the channel shows that the residues in the hydrophobic core of the bilayer are relatively more stable than those located close to the head group region and the aqueous phase. This may explain the unstable posi-

tion of the ion near the exit of the selectivity filter [27].

Since the potassium ions, which are localized in the selectivity filter, represent an integral part of the crystal structure, it is of interest to compare their possible locations as predicted by X-ray analysis [4, 6] to simulation findings. Based on the most recently published structure [6], it is conjectured that the  $K^+$  ions may occupy seven different locations : 4 inside the selectivity filter, one in the cavity and 2 ions weakly bound to the extracellular mouth. MD simulations, however, [11, 13, 27] indicate that only one or at most two ions may occupy the filter simultaneously. Some MD results report on only one ion in the filter, where second ion exits the filter either to the intracellular side [11] or to the extracellular side [27]. However, in the latter both cases, it cannot be excluded that the findings have to be attributed to incorrectly equilibrated structures. In particular, the results of the simulation [27] show that the potassium ion  $K_1$ , which originally binds to the oxygen atom of the Tyr<sup>78</sup> carbonyl group, finally dissociates into the aqueous phase. The  $K_2$ , which binds to the oxygen atom of the Thr<sup>75</sup> carbonyl group and  $K_3$ , which is located in the cavity, both remain bounded within the channel for the whole 3 ns of simulation. At equilibrium the  $K_2$  ion remains located between Gly<sup>77</sup> and Val<sup>78</sup>. Indeed, more elaborate simulations are necessary in order to clarify the details on ion localization in the selectivity filter.

The MD simulations predict an average number of water molecules within the cavity of about 21 [27], which is enough to solvate the cavity ion  $K_3$ , but which is in contrast to the conjecture of 50 water molecules based on solving the finite difference Poisson equation [28]. However, the latter result has to be viewed in the light of the recently reported shortcomings of the Poisson-Boltzmann theory applied to inhomogeneous systems [29].

## B PERMEATION

The goal of modelling the permeation process is to understand the physical processes underlying the permeation of ions through the channel, with the ability to reproduce present and predict future experimental observations. The time scale of permeation is too long to enable reproducing the experimental data on the process using MD calculations, so the modelling which attempts to reproduce experimental data usually employs more coarse-grained methods like continuum electrostatics and/or BD

simulations. Nevertheless, among the computational methodologies used on describing the permeation process, only molecular dynamics has the advantage of providing the data on the molecular kinetic details at the atomic resolution. However, none of the simulation studies with explicit lipid environment was able to complete the permeation process for the  $K^+$  ion within KcsA channel, due to the current computational limitations for simulations of such a large systems.

The permeation process deals with an open state conformation of the protein; the challenge for the theoretical approach is to explain the channel's ability to conduct the ion movement at very high rate and relate it to the detailed molecular structure of the system. In developing the realistic models of ion permeation, one is faced with remarkable complexities that need to be considered. 1) structure determinants of channel-mediated ion transport - the geometry of the protein-water interface along the permeation pathway, and 2) the distribution of charges in the protein wall, which determine ion-protein interactions along the pathway.

Although the precise geometry of ion-transport pathway varies among different channels, there are two characteristic regions that appear to be a general feature of all biological channels: a wider cavity that accommodates hydrated ion and short and narrow selectivity filter. Those two regions seem to be evolutionary conserved, at least in specific channel type (e.g. potassium channels).

The mechanism of ion permeation through the channel is generally determined by interactions of permeating ion with the channel wall and ion-ion interaction within the channel pore. Additionally, the interactions are modified with the physical determinants of water molecules within the narrow channel structure, that can be very much different from the bulk water outside the protein structure.

**Potential Energy Profile of KcsA.** The interaction energy of permeating ion with various constituents of the environment (e.g., water, protein, lipid, etc. ) is of considerable interest. In particular the interaction energy at various position along the axis of the channel (energy profile), give some indication for favorable positions of the ion. Energetic considerations for the KcsA channel have been reported previously [9, 26, 28] using free energy perturbation calculation or standard MD simulations of the channel without explicit environment. The complete energy profile including the contribution of a fully hydrated lipid bilayer membrane along the whole channel axis has

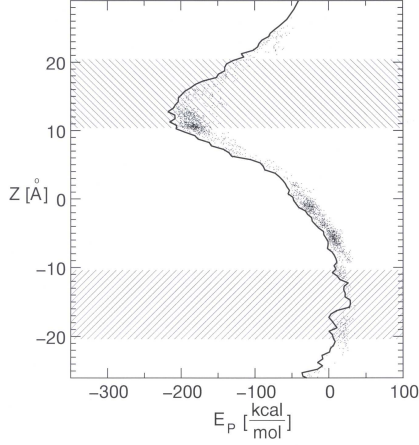


FIG. 1: Energy of a potassium ion interacting with the protein at different positions along the symmetry z-axis of the protein.

been reported recently [27]. The energy profile has been calculated using the non-equilibrium approach of steered molecular dynamics (SMD). This method was originally introduced in order to study the unbinding of the avidin-biotin complex [30, 31], but was shown to be a general tool to obtain equilibrium properties of a system from non-equilibrium measurements (proven recently by Jarzynski [32, 33]). In SMD, a restraint potential  $U_r(\vec{q}, t)$  is imposed on some degrees of freedom  $\vec{q} = (q_1, q_2, \dots, q_m)$  of the system, and is changed along specific paths. In the case of an ion channel, the external force pulls the ion by a spring attached to the ion along the channel's symmetry axis, quite similar as in the case of atomic force microscopy (AFM) experiments. The external potential is

$$U_r(x, t) = \frac{1}{2}k(x - vt)^2 \quad (2)$$

where  $x$  is the position of the atom,  $v$  and  $k$  are the speed and the spring constant of the cantilever, respectively. At time  $t = 0$  both the restraint center and atomic position are located at the same position. In Fig.1 the energy profile of the ion-protein interaction along the channel axis of KcsA is shown. A more detailed evaluation of other energy contributions from lipids, water and other ions inside the protein are presented in ref. [27]. The energy profile (Fig.1) exhibits a minimum at about 8 Å where the location of the first ion (K2) in the selectivity filter is, confirming experimental indications [6]. It has been

shown that the pore helices provide the most important contribution to stabilize the cavity ion, while the energetic barrier at the entrance of the intracellular side comes from the rest of the channel. Beside the calculation of the energy profile by means of SMD, it can be shown that the potential of mean force can be calculated as well, which is an important requisite for performing Brownian dynamics simulations [24] of a coarse-grained KcsA models.

**The Supplanting Mechanism in KcsA.** Several theoretical studies have addressed the multi-ion transport mechanism of permeation where several ions are located at the same time in cavity and selectivity filter. Since the kinetic details of the ion permeation are difficult to elucidate by experimental techniques, molecular dynamics simulation can play an important role in order to improve our understanding of ion permeation. Unfortunately, standard MD simulations, usually restricted to phenomena of a few nanosecond time scale, are not suitable to reproduce ion conduction taking place at tenths or hundreds of nanoseconds. Even for a high throughput channel as KcsA is, the experimentally measured ionic current of 10 pA gives the expected time of 16 ns to complete the permeation. However, applying an “alchemical” method [27] where water molecules and ions can exchange their places, the whole permeation process of a single ion can be monitored. The alchemical method can be considered as a variant of the “particle insertion” method, well known in computational physics [34]. In the particular case of the KcsA channel the permeation process due to multiple ions in the cavity region can be studied by this method. The potassium ion that escaped from the ion channel into the aqueous phase, exchanges its position with one water molecule in the cavity. This exchange process is taken, similar as in Monte Carlo simulations, with a probability proportional to  $\sim \exp[-\Delta U/k_B T]$  where  $\Delta U$  is the change in energy due to the exchange process,  $k_B$  the Boltzmann constant and  $T$  the temperature. In addition, the velocities of the water molecule and the ion under consideration are kept the same, hence rendering the kinetic energy unchanged during the exchange process. The orientational relaxation of cavity water molecules due to the introduction of the new ion is very fast, and the typical relaxation time is of the order of a few picoseconds. Several different locations in the cavity have to be taken as different initial positions for the permeation studies. The simulations are stopped at 500 ps, and a new position of the ion in the cavity is selected for a new trajectory. In many

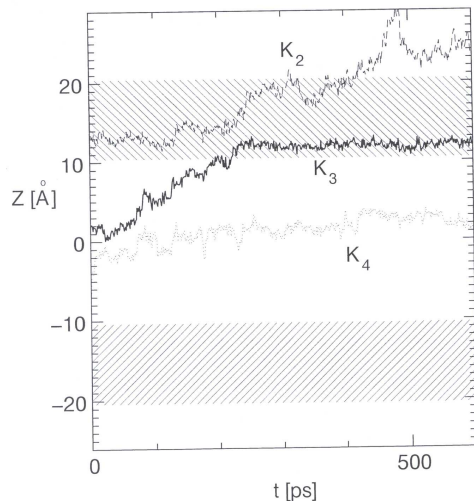


FIG. 2: Z-component of trajectories of three potassium ions as function of time. The ions K4 and K3 are initially located in the cavity within  $-5 < z < 7$ , the ion K2 in the selectivity filter at  $7 < z < 20$ . The shaded regions represent the head group regions of the POPC bilayer.

cases, the potassium ions do not enter the selectivity filter from the cavity. However, in some cases this event takes place. Fig.2 shows a typical example of the z-component of trajectories of three potassium ions as a function of time. The ions K4 and K3 are initially located in the cavity, which is in the range  $-5 < z < 7$ , and the ion K2 in the selectivity filter at  $7 < z < 20$ .

This result shows that the permeation process can be described by a “supplanting” process where the electrostatic repulsion between K3 and K4 leads to an expulsion of K3 into the selectivity filter, where it supplants the ion K2, which itself dissociates from the filter and moves into the extracellular mouth of the channel.

**Porins.** The existence of membrane water channels was predicted in the 1950s [35]. Today the detailed structures of several human [36] and bacterial [37] porins are known.

Bacterial porins from the outer membrane of *E.coli* allow diffusion of hydrophilic molecules with molecular weight up to 600 Da and exhibit modest ionic selectivity. The aqueous pore and the mechanism of ion conduction have been studied by MD simulations with explicit ions and solvent molecules [38]

and also with a lipid bilayer membrane [39]. The complete translocation of a single  $\text{Na}^+$  ion in the OmpF (outer membrane proteins in *E. coli*) under a potential of 500 mV was observed in 1.3 ns [38]. The simulation [39] revealed that a strong electric field oriented transversally to the pore axis influences the ion transport. The flow of one ion through various bacterial porins (OmpF, PhoE, OmpK36 and mutants thereof) has been studied using BD simulations [40–42] which show a good agreement between calculated transmission probabilities and experimental ion selectivity.

**Gramicidin.** Gramicidin A (gA), an antibiotic from *Bacillus Brevis*, has been for almost twenty years the only channel with a known structure, therefore presenting the favourite object for theoretical modelling. From physiological, as well as structural and functional point of view, it is not considered a biological channel. It is a 15-residue peptide, which forms a head-to-head dimer in the membrane, assuming a form of a 25 Å long cylinder with a central pore of 2 Å radius. The structure is permeant to monovalent cations ( $\text{H}^+$ ,  $\text{Li}^+$ ,  $\text{Na}^+$ ,  $\text{K}^+$ ,  $\text{Rb}^+$ ,  $\text{Cs}^+$ ), binds divalent cations and rejects all anions.

The featureless pore of gA is lined only by peptide backbone atoms, with symmetrical binding sites of moderate affinity near the entry and the exit. Alkali metal cation transport is considered, in simplest terms, to be carried out in three steps: two primarily extrachannel steps (diffusion through bulk aqueous solution up to the channel combined with entry into the binding site and exit from the exit site followed by aqueous diffusion away from the channel) and one intrachannel step (usually referred to as a cation translocation). The rate of the intrachannel step strongly depends on membrane potential, causing current-voltage relationships (I-Vs) to be superlinear when the intrachannel step is rate limiting. Thus I-Vs are sublinear at low permeant ion concentrations, where the extrachannel entry process is rate limiting, and become more superlinear with higher concentrations of permeating ion [43].

The permeation properties of gA channel seem to be also very dependent on the nature of the lipid environment (which is less likely to be the case for much larger, biological channels). Recently, some interesting results appeared on effects of membrane electrostatics on gA conductance properties. The data provided through experiments [44, 45] were, to a large extent, confirmed by continuum theory studies (3D Poisson-Nernst-Planck calculations) [46]. The calculated large changes in conductance of the chan-

nel (e.g. ionic current through gA is six fold larger in charged phosphatidylserine membrane than in a phosphatidylcholine membrane) caused by changed properties of the membrane (including lipid charges and dipoles, as well as membrane thickness) were consistent with experimental results.

Among other results obtained from simulations of gA, also some important aspects of  $H^+$  transport are revealed. Generally, proton fluxes across membranes constitute one of the most fundamental aspects of cell physiology, since the passive flow of  $H^+$  through  $H^+$  conducting channels drives ATP-synthesis. The non-equilibrium electrochemical potential for protons is achieved by  $H^+$  pumps (e.g. in bacteria, via bacteriorhodopsin, later discussed in the text) which utilize different forms of energy (from photochemical or redox reactions) to perform the uphill transport. Proton transport is postulated to occur via mechanism similar to one for salt-based conductivity suggested in 1805 by C. J. von Grotthuss [47] and therefore termed Grotthuss conductance. Within aqueous channels, proton transport occurs as covalent bonds exchange with hydrogen bonds between hydronium and a neighboring water to produce a charge transport, which is followed by a slower reorientation of the electroneutral water molecule.

Ion-free gramicidin channels contain eight or nine water molecules in a single file [43] which are free to interact and rotate. The water molecules thus form an ideal "proton wire", with fully aligned dipole moments as the lowest energy conformation. Channel permeability to protons is 40- to 60-fold higher than permeability to  $Na^+$ , and single-channel proton conductance at infinite dilution is 9.1-fold higher than  $Na^+$  conductance. Water flux is not induced by proton-mediated currents, as it is with alkali metal currents thus suggesting that  $H^+$  transport through the gA channel occurs by means of Grotthuss conductance [43].

A theoretical analysis of proton transport in a nine-water wire in vacuo emphasizes the difference between the time scales for proton passage ( $< ps$ ) and the subsequent water reorientation ( $> ns$ ) [48]. Positive charge transport first requires that a (hydrated) proton approach a channel containing a water column aligned with water oxygens toward the channel entry. After rapid exchange of hydrogen bonds and covalent bonds, which results in the release of a hydrogen at the channel exit, the water column has become aligned in the opposite direction and must completely reorient before the next proton transport can occur. Reorientation is expected to be rate-limiting and occurs by propagation of a

hydrogen-bonding defect through the channel. Furthermore, it is found that the mobility of  $H^+$  in the gramicidin channel is essentially determined by the fine structure and the dynamic fluctuations of the hydrogen-bonded network. The process of  $H^+$  permeation is mediated by thermal fluctuations in the relative positions of oxygen atoms in the wire. When permeating proton is not present, the water chain adopts one of the two polarized configurations, each corresponding to an oriented donor-acceptor H-bond pattern along the channel [49]. As the water molecules are ubiquitous in biological systems and form modulable H-bonded networks, it is expected that similar features in the coordination of these networks apply also to all the membrane proteins that provide efficient pathways for  $H^+$  transport.

## C SELECTIVITY

For every experimentally identified ion channel, there is a well defined ion selection sequence, according to which channels are usually named as potassium, sodium, chlorine or calcium channels. It appears that for the monovalent-selective channels the main selection criterion is the size of the ion, whereas for the calcium channel it is the magnitude of ion charge (calcium channel highly discriminates  $Na^+$  over  $Ca^{2+}$ , although the radii of  $Na^+$  and  $Ca^{2+}$  do not differ much - 0.95 vs. 0.99 Å, respectively). Thus, there are dominantly two different selection mechanisms at play; the one operates on the basis of ion size, and the other on the basis of ion charge.

The deciding factor on selectivity in channels is the free energy of permeation, namely the variation in free energy of the system as different ion species pass through the channel. In the simple case one can observe the differences in potential energies at various points along the pore, but for a more quantitative description, a free-energy calculations are needed.

**KcsA Channel.** The main focus of the MD simulations the KcsA potassium channel has been the selectivity filter and the permeation process from the cavity to the filter. The question of selectivity against  $Na^+$  ions has been addressed in several studies through free-energy perturbation calculations, where a  $K^+$  ion in one of the binding sites is alchemically transformed into a  $Na^+$  ion. The calculated free-energy barrier range from 11 kT to 8 kT [26], and 5 kT [25] which are in rough agreement with the experimental value of 9 kT extracted from the  $K^+/Na^+$  selectivity ratio of about  $10^4$ . It has been



found [26] that hydrophobic residues lining the intrapore and cavity are responsible for the relative high diffusion of ions in those segments. Despite the large suppression of the diffusion coefficient in the filter region, permeation through this segment has been found by BD simulations to be the fastest step in a full conduction cycle thanks to the Colomb repulsion. Recent MD simulation of Sansom and coworkers [50] indicate that  $K^+$  ions and water molecules within the filter undergo concerted single-file motion in which they translocate between adjacent sites within the filter, on a nanosecond time scale. In contrast,  $Na^+$  ions remain bound to the sites within the filter and do not exhibit translocation. Furthermore, the entry of a  $K^+$  ion into the filter from the extracellular mouth is observed, whereas this does not occur for a  $Na^+$  ion. It is argued [50] that these differences in interactions in the selectivity filter may contribute to the selectivity of KcsA for  $K^+$  ions in addition to the differences in the dehydration energy between  $K^+$  and  $Na^+$  and the block of KcsA by internal  $Na^+$  ions. A more direct evidence for the selectivity against  $Na^+$  has been obtained using the alchemical MD [27].

**$Ca^{2+}$  Channels.** Our understanding of ion permeation and selectivity in calcium channels is still poor. In the absence of a molecular sieve mechanism which selects between ions on the basis of ionic radii, reconciling their high selectivity and high conductance has been a difficult problem. Calcium channels are very selective against  $Na^+$  ions and exhibit a multi-ion Coulomb repulsion mechanism to achieve a high conduction of  $Ca^{2+}$  ions. The fact that the two ions have similar radii but different charges indicates that selectivity must be based on charge. Since the detailed structure of a calcium channel is not available, Chung and coworker [51] have studied a coarse-grained model using BD simulations. They have used the available information on the structure and conductance properties to construct a model channel consisting of inner and outer vestibules and a selectivity filter. The filter was designed such that two critical elements, its size and charges on its wall, were determined from experimental data. The radius was set to 2.8 Å according to the size of tetramethylammonium, the largest permeable ion. Four negatively glutamate residues were assigned to the filter region. The BD simulations have quite successfully reproduced experimental current-voltage curves, saturation of conductance with concentration, selectivity against  $Na^+$ , the anomalous mole fraction effect, attenuation of the calcium current by external sodium

ions, and the effect of mutating glutamate residues on blocking of sodium current.

**Porins.** The extraordinary permeation rate of 3 billion water molecules per second per single aquaporin-1 (AQP1) molecule, combined with the strict selectivity for water, have challenged several MD simulations in order to elucidate the relation between structural determinants and selectivity [52–55].

The MD simulations of the protein tetramer for several nanoseconds [53] reveal that the water molecules are strongly oriented in the channel interior with their dipoles rotating by about 180° during permeation. The dipoles are aligned with the electric field which originates from the dipoles of two specific helices, HB and HE, of the protein. Hydrogen competition between water molecules and a few polar groups in the pore was found to dominate the permeation process.

Hydrogen bond statistics for water molecules show that there are two major interaction sites inside the channel: the Asn-Pro-Ala (NPA) region and the aromatic-arginine (Ar/R) constriction region. The two highest enthalpic barriers to the passage of water molecules are located directly adjacent to NPA region. This, together with the water rotation which also occurs here, suggest that the NPA region is a major selectivity filter.

Porins are often designed such that proton conduction is strictly prevented in order to maintain the proton gradient across the cell membrane which serves as a major energy storage mechanism. In the simulations, frequent simultaneous hydrogen bonding of water molecules to the two NPA asparagines has been observed, thereby weakening interactions among adjacent water molecule in the pore. As contiguous hydrogen bonded water chains are known to be efficient proton conductors, it was suggested that this region is the main proton filter [55].

## D GATING

Ion channels regulate the selective transfer of ions across the membrane in response to different types of stimuli, as e.g. changes of pH, transmembrane potential, mechanical stress or ligand binding. A channel can generally assume two stable conformations, the open and the closed one. The structural part of the channel responsible for the gating controls the accessibility of ions to a centrally located water-filled pore. The opening and closing of the gate is accompanied by conformational changes in the protein

during gating. The structural and dynamical details of the gating mechanism are the least known properties of ion channels, mostly because of the fact that an opened state of the channel is a transient one, thus not easily fixed to be isolated by crystallization. Consequently, for the majority of known structures no direct comparison of X-ray structures is available and one has to get to other experimental techniques that suggest the structural determinants of the gating mechanism.

**The KcsA Potassium Channel.** The *Streptomyces lividans* potassium channel (KcsA) is pH regulated [56]. A gating mechanism was proposed by Perozo and coworkers [57–59] by using the site-directed spin-labeling methods and electron paramagnetic resonance spectroscopy. Results from these experiments indicate that the channel undergoes a “twisted” motion where each of the four TM2 helices tilts away from the permeation pathway, towards the membrane plane, and rotates about its helical axis, supporting a scissoring-type motion with a pivot point near residues 107–108. These movements result in a large increase of the diameter of the intracellular mouth up to the central water-filled cavity. Although the possible collective motion of the helices can be constructed, mainly based on steric considerations, the origin of the pH-mediated driving force is still unclear. It has been conjectured [60] that the four long cytoplasmic C-termini of residues 123–160 may play the crucial role, because some of the charged residues may change their protonation state during pH variation and hence provide the necessary variation in their inter-chain Coulomb interaction. Another candidate for pH-mediated conformational transitions are the four N-termini 1–23 carrying also titrable groups. It is unclear how these chains interact with each other, possibly indirectly with the lipid head groups of the membrane which are in general pH sensitive. Unfortunately the gating mechanism cannot be studied by standard MD simulation because the time scale of gating is in the order of at least microseconds. The simulation of the channel gating is therefore still one of the great challenges in biophysics.

**Mechanosensitive Channels.** MscL, a bacterial mechanosensitive channel of large conductance, is the first structurally characterized mechanosensor protein [61–64]. The protein is a pentamer, approximately 50 Å wide in the plane of the membrane and 85 Å tall. Each 151-residue subunit consists of two transmembrane helices, labeled TM1 and TM2, and

a cytoplasmic helix that extends some 35 Å below the membrane. The TM1 helices are arranged so as to block diffusion through the channel at their N-terminal ends. Excision of the cytoplasmic domains has been found to have little effect on the gating properties of the channel. In prokaryotes the channel plays a crucial role in exocytosis and in response to large osmotic pressure changes. In general, it is believed that the gating of mechanosensitive channels is induced by changes in the intra-bilayer pressure profiles which originate from bilayer deformation. In order to change the membrane tension, it has been suggested [63] that different hydrophobic mismatches at the protein-lipid interface induced by different types of lipids may cause an asymmetry of tension across the bilayer membrane and hence lead to a spontaneous curvature which controls the open and the closed state. At least, it is clear from experiments with different types of mixtures of lipids [63, 64] that the protein-lipid interaction must play a fundamental role in defining the physical principles that underly MscL gating.

Recently, MD simulations [65, 66] have been performed in order to contribute to the experimental data on gating mechanism. Standard MD simulation in the nanosecond time regime and the analysis of the structural fluctuations have indicated that the least mobile part of the protein could be identified as the gate, on the same location as it was suggested by the experimental findings. This part comprises the first 5 residues of the TM1 helices, which are shown to be pinched together to form a non-leaky occlusion. In addition, steered MD simulation [65] of the bare protein without membrane and without water has been carried out. The effect of the membrane on the protein has been taken into account by applying a constant surface tension on the protein. Under a range of conditions, it has been shown that the transmembrane helices tilted considerably as the pore opened. The protein refolded into an open conformation, where the transmembrane helices flattened as the pore widened, with a minimal loss of secondary structure. The rate at which the protein refolded has been nearly inversely proportional to the applied surface tension. The results indicate that membrane thinning and hydrophobic mismatch within the transmembrane helices may indeed drive gating.

### III. MEMBRANE PUMPS

In the following section we report on some recent progress in modeling and simulating active transport processes across bilayer membranes. Here we restrict our attention to the case of membrane protein bacteriorhodopsin, which serves as a light driven proton pump in bacterial cells.

The protein bacteriorhodopsin (bR) resides in the membrane of the archaeobacterium *Halobacterium salinarum* and uses photonic energy for transmembrane proton pumping. Proton transport is a critical process in physical chemistry and biology, including ATP production voltage-activated proton channels in epithelia and light transduction. The protein incorporates a retinal chromophore bound to a lysine residue via a protonated Schiff base linkage and absorbs light around 568 nm. Photoexcitation triggers an isomerization of retinal. The photoreaction induces a vectorial transfer of a proton across the membrane, leading to the release of a proton at the extracellular side and an uptake from the cytoplasmic side. Our current knowledge of the structure and the photocycle of bR has been reviewed in detail by several authors [67–69]. In particular, since certain dynamical features of bR cannot be captured by crystallographic techniques, molecular dynamics simulations have been used to elucidate, among others, conformational fluctuations [70–72] and bR-water mobility [73, 74].

Although the molecular structure of bR in its ground state is now well determined, details of intermediate photocycle states are still controversial [75, 76]. In addition, the amount of buried (“internal”) water molecules in bR [77–80] which are assumed to play a decisive role in providing proton pathways and to be involved in the molecular mechanism leading to proton translocation, is still unclear.

Very recently [81] new details of the amount and the distribution of internal water molecules, and of the related hydrogen-bonded networks in bR that constitute proton pathways, has been reported. This work provides important information on hydrogen-bonded networks in bR fluctuating on the ps to ns time scale, which has not been seen in crystallographic studies.

**Distribution of Water Molecules.** Using molecular dynamics simulations the number of internal water molecules in bR have been estimated. In addition, “diffusive” and “trapped” water molecules have been discriminated. From the simulations, the average number of diffusive water has been estimated to 24.

The average fluctuation is about 1.5. The equilibrium distribution of internal water molecules (IWM) in bR is shown in Fig.3. The number density  $n_w(z)$  has been calculated with respect to the  $z$ -axis, i.e., the average number of IWM within a slab of thickness  $\delta z = 1 \text{ \AA}$ . The origin  $z = 0$  is placed at the center of mass of the protein. Strictly speaking, the notion “diffusive” IWM has to be defined more precisely. There are many water molecules entering the protein very transiently, i.e., crossing the “mathematically” defined protein surface and penetrating up to a few  $\text{\AA}$  before exiting again. Those “surface” water molecules do not perform an actual diffusion inside the protein over an substantial amount of time. Therefore, in the data of Fig.3 only those IWM have been included, which have spent more than 10 ps inside bR. Only in this case, the analysis of the simulation data yields an average of 24 IWM. Without this restriction, i.e., including the “surface” water molecules, the average of diffusive IWM is approximately 80.

The first remarkable information from the distribution  $n_w(z)$  is that a migration of water between the extracellular and cytoplasmic part does not take place within the simulation time. This is concluded from the gap in the distribution of diffusive molecules. This gap reflects a kind of structural “watershed” in the protein. The existence of this impenetrable structural interface between the cytoplasmic and the extracellular part of bR was already concluded from crystallographic data and is a necessary feature of the protein in its ground state, prohibiting a spontaneous transport of protons across the membrane.

The distribution of IWM (diffusive and trapped), as detected by crystallographic data and as found during our simulations, have been compared recently [81]. Both distributions are in qualitative agreement as far as the overall shape is concerned : less water molecules near the center of the protein, more outside. However, from the quantitative point of view, they differ considerably. The crystallographic data of Sass et al. [75] contain in total 77 water molecules, out of which only 18 are inside the protein, whereas the simulation data provide a much higher amount of IWM, 44. Integration of  $n_w(z)$  obtained by simulation leads to an average of 44 water molecules inside the protein, out of which are 24 diffusive and 20 trapped. It is also interesting to note that the average number of internal water molecules in the cytoplasmic domain, 25, is higher than in the extracellular one, 19.

The explanation for the large discrepancy of the

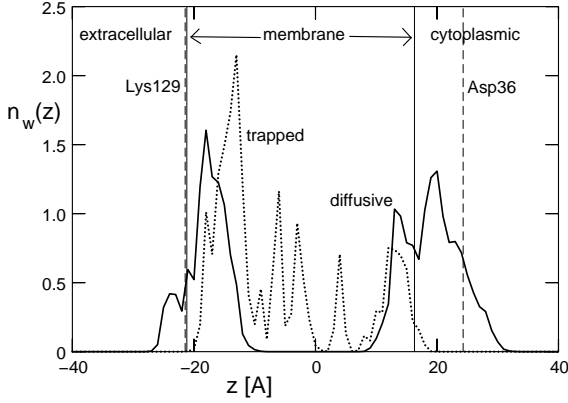


FIG. 3: One-dimensional number density  $n_w(z)$  of water molecules in bR as found by simulation. The full and the dotted lines denote diffusive and trapped water molecules, respectively. The two full vertical lines denote the average positions of the two membrane surfaces defined by the average locations of the nitrogen atoms of the lipid head groups. The two broken vertical lines indicate the average positions of the  $\alpha$ -carbon atoms of Asp36 and Lys129 which are located close to the surface of bR.

number of IWM, as found during simulation and as compared to the crystallographically found IWM, is the high exchange rate of water molecules between internal and external locations. Therefore, it is of interest to characterize some time-dependent properties of IWM in terms of typical residence times and correlation times. This can be performed using simulation data. Consider a particular ensemble of IWM at a certain time  $t$ . For this ensemble one can define the "exchange" (or turn-over) time  $\tau_{ex}$  as the time after which all IWM of this ensemble have been replaced by new IWM. The average decay of such an ensemble is described by  $N_w^{(e)}(t)$ , as the average number of remained IWM of an ensemble after time  $t$ , follows an exponential law at larger time according to

$$N_w^{(e)}(t) \sim \exp(-t/\tau_{cor}), \quad t > 100 \text{ ps} \quad (3)$$

where the correlation time  $\tau_{cor} \approx 180$  ps characterizes the time evolution of the "exchange" process of those IWM which penetrate deeply into bR. At shorter times,  $t < 50$  ps, there are rapid exchange processes which are due to the "surface" water molecules which do not perform a diffusion inside

bR before exiting, and hence  $N_w^{(e)}(t)$  decreases in this time regime much more rapidly than at larger times. One implication from the typical time scales  $\tau_{ex}$  and  $\tau_{cor}$  is, that due to exchange processes of IWM on a time scale of a few 100 ps, it is very difficult to detect by crystallographic methods the accurate amount of water molecules inside bR. A second quantity, which corroborates this view and which characterizes the dynamics of diffusive IWM, is the distribution of residence times in a given ensemble of IWM. The residence time  $\tau_{res}$  is the time which one of the diffusive IWM spends inside the protein. Then,  $N(\tau_{res})$  is the number of IWM with residence time  $\tau_{res}$  found in a given ensemble of diffusive IWM. The average over many ensembles, taken from simulation data, exhibits a distribution of  $N(\tau_{res})$  which is well described by a power law within a certain time range of  $1 < \tau_{res} < 300$  ps,

$$N(\tau_{res}) \sim (\tau_{res})^{-1}, \quad 1 < \tau_{res} < 300 \text{ ps}. \quad (4)$$

From this distribution  $N(\tau_{res})$  the average residence time of a water molecule has been calculated to  $\langle \tau_{res} \rangle \approx 52$  ps. Again, this result explains why it is very difficult to detect the accurate amount of water molecules inside bR by crystallographic methods.

**Structure of Hydrogen-Bonded Network.** During the photocycle, protons are vectorially transported from the cytoplasmic side to the extracellular environment. During this process the proton is captured by the Schiff base of the retinal group. This implies that hydrogen-bonded pathways must exist between the cytoplasmic surface of the protein and the Schiff base via the side chain Asp96 as shown by infrared spectroscopy.

With regard to the previous section, which is concerned with the water population in bR, we now address the question about the quantitative contribution of water molecules to generate hydrogen-bonded pathways between the bR's aqueous environment and the core of bR. We have considered the following constructs of hydrogen-bonded chains.

The hydrogen-bonded pathway is related to the "Grotthuss relay mechanism" for proton transport. Since there is a vast amount of literature on this subject, we simply quote a few and more recent articles [47, 82–84]. There, the ordered chains of water molecules are considered, where one path consists of an alternating sequence of hydrogen bonds between water molecules,  $\text{H} \cdots \text{O}$ , separated by  $\text{O}-\text{H}$  bonds of water molecules. In this case, the protons are assumed to hop in a rate-limiting process along such a path which results in a reorientation

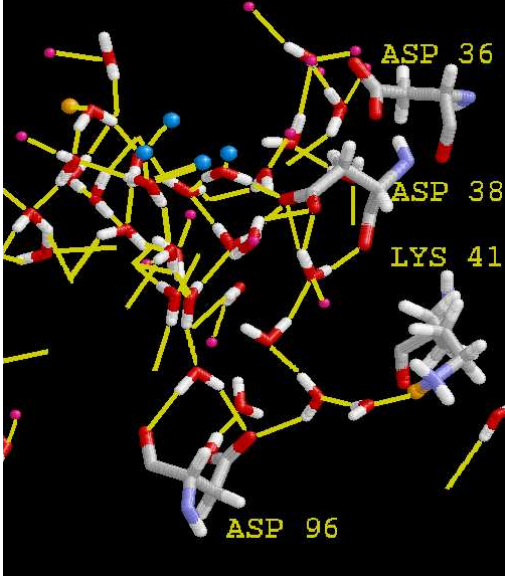


FIG. 4: Snapshot of a hydrogen-bonded network connecting the protein surface and Asp96. The yellow lines denote hydrogen bonds. The blue balls denote external water molecules to which Asp96 is connected via hydrogen bonds. Pink balls denote water molecules to which Asp96 is not connected. Orange balls denote other residues not denoted in the figure.

of the participating water molecules. Many refinements of this model have been proposed [85]. In spite of the simplicity of the Grotthuss model, its application, in particular to biological systems, has lead to many valuable insights into proton transport governed by the concerted actions of spontaneously forming hydrogen-bonded networks and the structural fluctuations of the embedding proteins [86, 87]. In the recent study [81], however, the Grotthuss-path model was used as a static geometrical construct rather than a dynamical one. A dynamical picture would include certain time-dependent correlations between proton and water displacements. However, using a static picture, this approach can be considered as a description of the capability of bR to form spontaneously Grotthuss-pathways which are relevant for proton transport. In Fig.4 we have depicted a typical snapshot of a hydrogen-bonded network connecting the protein surface and Asp96.

It is of interest also to characterize the average geometry of the hydrogen-bonded networks targeted to Asp96. It has been shown [81] that the distribution of bonds are localized in a certain regime. Consid-

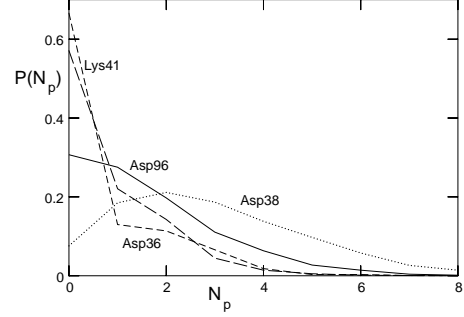


FIG. 5: Probability distribution  $P(N_p)$  of the number  $N_p$  of hydrogen-bonded pathways connecting at the same time various amino acids to the protein surface. For simplicity we have included only pathways consisting solely of water molecules (Grotthuss pathways).

ering the fairly large, less compact bond distribution near the surface of the protein, one may speculate that the hydrogen-bonded network targeted to Asp96 works as a kind of “funneling” requisite. A more quantitative description of the network is presented in the following figures 5 and 6.

In Fig.5, the probability distribution  $P(N_p)$  of the number  $N_p$  of hydrogen-bonded pathways connecting at the same time various amino acids to the protein surface is shown. For simplicity we have included only pathways consisting solely of water molecules (Grotthuss pathways). Since the probabilities for various amino acids at  $N_p > 2$  are significantly  $P(N_p) > 0$  (e.g. Asp96 and Asp38,  $P(N_p=5) > 0.1$ ), this result demonstrates that for various side chains many hydrogen-bonded pathways to the protein surface can exist at the same time.

The average number  $N_G(L)$  of Grotthuss paths consisting of  $L$  hydrogen bonds is shown in Fig.6. These pathways connect the protein surface to various types of amino acids in the cytoplasmic half of the protein. The average length of a Grotthuss-path (in units of a hydrogen bond) is given by  $\langle L \rangle = \sum_L L N_G(L) / \sum N_G(L)$ , and calculated to  $\langle L \rangle = 6.0, 4.1, 5.1, 4.8$  for Asp96, Lys41, Asp38, and Asp36, respectively. The quantity  $N_G(L)$  has been calculated from 250 snapshots of the system during the 2.5 ns simulation time, i.e., every 10 ps. At each snapshot, the number of Grotthuss paths of length  $L$  has been calculated and added to  $N_G(L)$ . The final result was then normalized by 250. The average

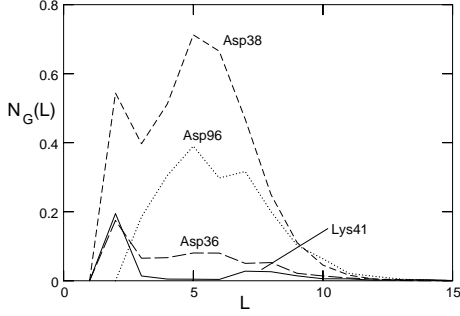


FIG. 6: Average number of Grotthuss pathways  $N_G(L)$  as a function of path length  $L$  which is the number of hydrogen bonds connecting a particular amino acid to the protein surface. Given for various amino acids, as indicated.

number of Grotthuss pathways is  $\langle N_G \rangle \approx 2$ .

**Dynamics of Hydrogen-Bonded Network.** Each hydrogen-bonded path is transient and exists only for a certain life time. Since these paths are assumed to constitute proton pathways, it is important to estimate their life times which can provide some insights into the efficiency of the proton translocation.

During the simulation we have monitored various hydrogen-bonded pathways connecting certain residues, as potential proton acceptors, to the protein surface. A pathway of any length  $L$  is considered to be broken if any one of its constituting hydrogen bonds is broken. The corresponding life time  $\tau_p$  is then stored in a histogram which finally provides the probability density distribution  $P_L(\tau_p)$ . The result for cytoplasmic pathways is shown in Fig.7 for  $2 \leq L \leq 13$ . From the data one can calculate the average lifetime  $\langle \tau_p \rangle = \sum_L \sum \tau_p P_L(\tau_p)$ , which yields approximately  $\langle \tau_p \rangle = 0.045$  ps. The probability distribution  $P_L(\tau_p)$  can be described approximately by a stretched exponential for  $\tau_p > 0.01$  ps,

$$P_L(\tau_p) = c_L \exp[-\sqrt{\tau_p/b}], \quad (5)$$

where  $b = 0.0073$ , and  $c_L$  is a constant depending on  $L$ : 3.1, 6.5, 9.7, 9.8, 11.4, 7.6, 5.0, 2.7, 1.1, 0.97, 0.40, for  $3 \leq L \leq 13$ . This is demonstrated in Fig.8 where the semi-log plot of the  $\sum_L P_L(\tau_p)$  versus  $\sqrt{\tau_p}$  shows the stretched exponential over one order of magnitude in time.

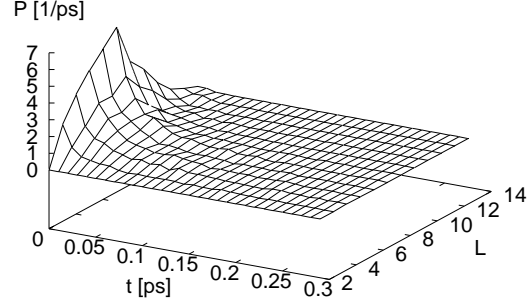


FIG. 7: Probability distribution  $P_L(\tau_p)$  of the life-times  $\tau_p$  of hydrogen-bonded pathways connecting the protein surface and Asp96.

Since it is well known that re-protonation of Asp96 takes several ms [88, 89], it is of interest to correlate this time to the probability distribution  $P_L(\tau_p)$ . It is known that the proton hopping time  $\tau_H \approx 1.5$  ps [90] between hydronium and water accounts for the abnormal proton mobility if one assumes that hopping takes place across a *single* water molecule at a time. Assuming the applicability of the Einstein relation for diffusion along a one-dimensional path

$$a_H^2 = 2 D \tau_H \quad (6)$$

one can estimate a reasonable diffusion coefficient by assuming a hopping length of  $a_H = 2.5$  Å, which is the hydrogen-bond length between water and  $\text{H}_3\text{O}^+$  [47, 91]. The calculation gives  $D = 2.1$  Å<sup>2</sup>/ps. Assuming a hydrogen-bonded pathway of length  $L = 5$ , then the proton would need on the average a time of  $\tau_L = (L a_H)^2 / 2D \approx 37$  ps to travel along a path between protein surface and Asp96. According to Eq.5 the probability to find a pathway existing for a traveling time  $\tau_L$  is the sum over all probabilities  $P_L(\tau_p)$  for  $\tau_p \geq \tau_L$ . Integration of Eq.5 yields

$$\tilde{P}_L(\tau_L) \equiv \int_{\tau_L}^{\infty} P_L(x) dx = 2 c_L b \exp[-\sqrt{\tau_L/b}] (\sqrt{\tau_L/b} + 1). \quad (7)$$

Then the waiting time for a proton to travel a distance of  $L$  is in the order of

$$\tau_{wait} \approx \frac{\langle \tau_p \rangle}{\tilde{P}_L(\tau_L) \langle N_G \rangle}. \quad (8)$$

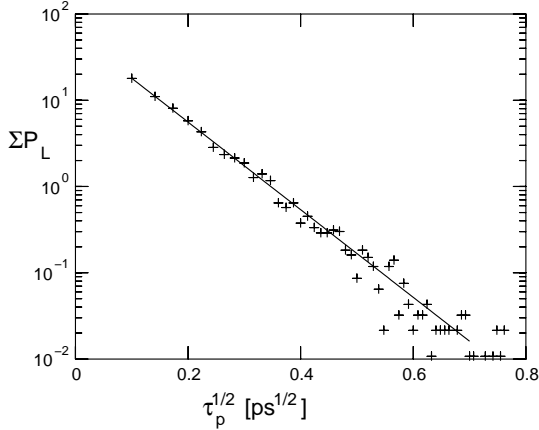


FIG. 8: Semi-log plot of the sum of the probabilities  $\sum_L P_L(\tau_p)$  of the lifetimes  $\tau_p$  of hydrogen-bonded pathways versus  $\sqrt{\tau_p}$ . The crosses represent the same data as given in Fig.7.

This is shown in Fig.9 where the waiting time is plotted as a function of the traveling time  $\tau_L$ . From Fig.9 it is obvious that  $\tau_L = 37$  ps leads to an unreasonably long waiting time which excludes the possibility of a diffusional proton translocation between the protein surface and Asp96.

The key problem is the long traveling time  $\tau_L$ . This time, however, would be much shorter if local electric fields due to the surrounding residues would induce a drift of the proton along the path and along the direction of the electric field according to

$$v = \mu_H E \quad (9)$$

where  $v$  is the proton drift velocity,  $\mu_H = 36 \text{ \AA}^2/\text{V ps}$  the proton mobility [90], and  $E$  the internal electric field strength. Assuming a field in the order of the membrane electric field  $E = 0.05 \text{ V/\AA}$  (see e.g. [92]) yields  $v = 1.8 \text{ \AA/ps}$ . Interestingly, the effective velocity of a proton hopping process  $v_H = a_H/\tau_H = 1.67 \text{ \AA/ps}$  is in the same order of magnitude, which indicates that probably the electric field does not effect very much the hopping process, but rather works as a rectifier. From the drift relation between displacement and time

$$L a_H = v \tau_L \quad (10)$$

one obtains, e.g., for  $L=4$ , and  $L=5$  traveling times  $\tau_L = 5.5$  ps and  $\tau_L = 6.9$  ps, respectively. According to Fig.9 these numbers yield waiting times  $\tau_{wait}$  of 8

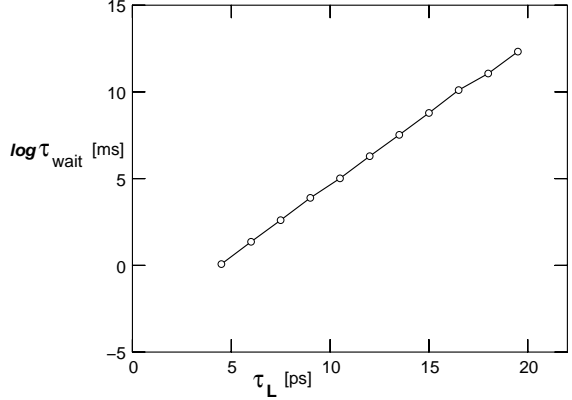


FIG. 9: The logarithm of the waiting time  $\log \tau_{wait}$  versus traveling time  $\tau_L$ .

ms and 124 ms, respectively, which are in reasonable agreement with experiments.

The internal electric fields in the cytoplasmic domain of bR are unknown. But similar as in the extracellular domain of bR where the proton reaction transfer is driven by a set of pK shifts, and hence by changes of local electric fields that propagate along the proton-conducting path, a corresponding mechanism may work during the proton translocation in the cytoplasmic side of bR as well. Therefore it would be of interest to investigate the internal electric fields of bR, that are of particular interest for intermediate states during the photocycle of bR [93].

#### IV. OUTLOOK

A good theoretical model of the membrane protein has to relate the structure to its function. The ultimate approach to the structure-function problem is expected to be molecular dynamics simulation, since it is the only present computational method that treats all parts of the system explicitly. Unfortunately, present state of the computational speed is far beyond this goal: for the membrane channels, it is still not possible to calculate most of the properties within a reasonable time, even employing the largest and fastest computers. On the other hand, MD approach calls for a high resolution data on membrane protein structure, which is still a rare case to find.

Nevertheless, a judicious use of experimental clues can help developing a simplified models of ion chan-

nels that could be sufficiently accurate for the purposes of electrostatic continuum calculations and BD simulations, which can provide the output data on conductance, reproduce I-V curves, etc. Those coarse-grained models would still be of a value, specifically in the cases where environmental effects on functional properties are to be evaluated. Also, a development in proper integration of coarse-grained with atomistic approaches is expected.

One of the challenges for future modelling efforts would surely be in including more detailed description of the system, specifically in the environmental conditions for the membrane proteins. The reasons for this expectation comes from various directions which emphasise the importance of protein-lipid interactions.

The protein-lipid interaction can, at least in some cases, produce a modulation of membrane protein function itself. As the reported example of gramicidin A shows, the electrostatics and geometry of surrounding lipids can have a profound influence on channel properties. Although this influence is expected to be larger for such a small channels as gA is, it should not be underestimated also in the case of real, biological channels as well. The profound effect of lipid environment on the structure and function of nACh receptor channel is recently experimentally shown [94]. However, it has been long known that a large number of membrane proteins is selective towards specific membrane lipids, indicating that membrane proteins call for a specific lipid environment in order to function properly. Moreover, in order to resolve the need for presence of non-bilayer lipids for normal physiological functioning in variety of cells, it has been suggested that the presence of non-bilayer forming lipid class is crucial for ensuring the physiologically functional conformation of the membrane proteins via the specific lipid-protein interactions [95, 96]. Confirming of that is the example of gating regulation for MscL channel through varying the lipid composition, including the presence of non-bilayer forming lipids.

Another problem that would have to be encountered in future simulation attempts is a higher level of complexity in protein structure. Simulations of membrane proteins so far considered just a pore defining domain of the protein structure. The reported example of membrane proton pump bacteriorhodopsin, which is modelled in simulations as a monomer, naturally in membranes occurs as trimer. Some recent calculations suggest that structural changes of the pore domain appear in conformation of trimer vs. monomeric form. Additionally,

some membrane proteins can be found in diversity of conformations (monomeric or multimeric conformations, homomeric as well as heteromeric structures), which can produce functionally different entities, as in the example of KCNQ family of channel proteins [97], suggesting the necessity of including complete structures in computational simulations. Some classes of  $K^+$  channels as well as nACh membrane channel, also include water-soluble domains or subunits, which may alter channel properties [98–100], thus presenting the need of including those structures in the future calculations as well.

## REFERENCES

- [1] Urry, D.W. 1971. The gramicidin A transmembrane channel: a proposed  $\pi_{LD}$  helix. *Proc. Natl. Acad. Sci. USA* 68:672-676.
- [2] Partenskii, M.B., Jordan, P.C. 1992. Theoretical perspectives on ion-channel electrostatics: continuum and microscopic approaches. *Q. Rev. Biophys.* 25:477-510.
- [3] Roux B., Karplus M. 1994. Molecular dynamics simulations of the gramicidin channel. *Annu. Rev. Biophys. Biomol. Struct.* 23:731-761.
- [4] Doyle, D.A., J. Morais-Cabral, R.A. Pfuetzner, A. Kuo, J.M. Gulbis, S.L. Cohen, B.T. Chait, and R. MacKinnon. 1998. The structure of the potassium channel: Molecular basis of  $K^+$  conduction and selectivity. *Science* 280:69-77.
- [5] Morais-Cabral, J.H., Y.F. Zhou, and R. MacKinnon. 2001. Energetic optimization of ion conduction rate by the  $K^+$  selectivity filter. *Nature* 414:106-109.
- [6] Zhou, Y.F., J.H. Morais-Cabral, A. Kaufman, and R. MacKinnon. 2001. Chemistry of ion coordination and hydration revealed by a  $K^+$  channel-Fab complex at 2.0 Å resolution. *Nature* 414:106-109.
- [7] Jiang, Y., A. Lee, J. Chen, M. Cadane, B.T. Chait, and R. MacKinnon. 2002. The open pore conformation of potassium channels. *Nature* 417:523-526.
- [8] Valiyaveetil, F. I., Y. Zhou, and R. MacKinnon. 2002. Lipids in the structure, folding, and function of the KcsA  $K^+$  channel. *Biochemistry* 41:10771-10777.
- [9] Allen, T.W., S. Kuyucak, and S.-H. Chung. 1999. Molecular dynamics study of the KcsA potassium channel. *Biophys. J.* 77:2502-2516.
- [10] Guidoni, L., V. Torre, and P. Carloni.



1999. Potassium and sodium binding to the outer mouth of the  $K^+$  channel. *Biochemistry* 38:8599-8604.
- [11] Shrivastava, I.H., and M.S.P. Sansom. 2000. Simulations of ion permeation through a potassium channel: Molecular dynamics of KcsA in a phospholipid bilayer. *Biophys. J.* 78:557-570.
- [12] Guidoni, L., V. Torre, and P. Carloni. 2000. Water and potassium dynamics inside the KcsA  $K^+$  channel. *FEBS Lett.* 477:37-42.
- [13] Bernéche S., and B. Roux. 2000. Molecular dynamics of the KcsA  $K^+$  channel in a bilayer membrane. *Biophys. J.* 78:2900-2917.
- [14] Bernéche S., and B. Roux. 2001. Energetics of ion conduction through the  $K^+$  channel. *Nature* 414:73-77.
- [15] Lu, Z., A.M. Klem, Y. Ramu. 2001. Ion conduction pore is conserved among potassium channels. *Nature* 413:809-813.
- [16] LeMasurier, M., L. Heginbotham, C. Miller. 2001. KcsA: it's a potassium channel *J. Gen. Physiol.* 118:303-313.
- [17] Hille B. 2001. Ion channels of excitable membranes. Third Edition. Sinauer Associates inc. Sunderland, Massachusetts, Third e.
- [18] Aidley, D.J., and P.R. Stanfield, Ion channels: Molecular inaction, (Cambridge University Press, Cambridge, 1996).
- [19] MacKinnon, R., S.L. Cohen, A. Kuo, A. Lee, B.T. Chait. 1998. Structural conservation in prokaryotic and eukaryotic potassium channels. *Nature* 280:106-109.
- [20] Kuyucak, S., S. Andersen, S.-H. Chung. 2001. Models of permeation in ion channels. *Rep. Prog. Phys.* 64:1427-1472.
- [21] Tieleman, D.P., P.C. Biggin, G.R. Smith, M.S.P. Sansom. 2001. Simulation approaches to ion channels structure-function relationships. *Q. Rev. Biophys.* 34:473-561.
- [22] Roux, B. 2002. Theoretical and computational models of ion channels. 2002. *Curr. Opin. Struct. Biol.* 12:182-189.
- [23] Neher, E. and B. Sackmann. 1976. Single-channel currents recorded from membrane of denervated frog muscle fibres. *Nature* 260:799-802.
- [24] Chung, S.-H., T.W. Allen, M. Hoyles, and S. Kuyucak. 1999. Permeation of ions across the potassium channel: Brownian dynamics studies. *Biophys. J.* 77:2517-2533.
- [25] Åqvist, J., and V. Luzhkov. 2000. Ion permeation mechanism of the potassium channel. *Nature* 404:881-884.
- [26] Allen, T.W., A. Bliznyuk, A.P. Rendell, S. Kuyucak, and S.-H. Chung. 2000. The potassium channel: Structure, selectivity and diffusion. *J. Chem. Phys.* 112:8191-8204.
- [27] Lin, J.-H., J.-F. Gwan, and A. Baumgaertner. 2002. Selective ion permeation in a potassium ion channel with a flexible selectivity filter. (preprint 2002)
- [28] Roux B. and R. MacKinnon. 1999. The cavity and pore helices in the KcsA  $K^+$  channel: Electrostatic stabilization of monovalent cations. *Science* 285:100-102.
- [29] Moy, G., B. Corry, S. Kuyucak, S.-H. Chung. 2000. Tests of continuum theories as models of ion channels. I. Poisson-Boltzmann theory versus Brownian dynamics. *Biophys. J.* 78:2349-2363.
- [30] Grubmüller, H., B. Heymann, and P. Tavan. 1996. Ligand binding: Molecular mechanics calculation of the streptavidin-biotin rupture force. *Science* 271:997-999.
- [31] Izrailev, S., S. Stepaniants, M. Balsera, Y. Oono, and K. Schulten. 1997. Molecular dynamics study of unbinding of the avidin-biotin complex, *Biophys. J.* 72:1568-1581.
- [32] Jarzynski, C. 1997. Nonequilibrium equality for free energy differences. *Phys. Rev. Lett.* 78:2690-2693.
- [33] Jarzynski, C. 1997. Equilibrium free-energy differences from nonequilibrium measurements: A master-equation approach. *Phys. Rev. E.* 56:5018-5035.
- [34] Widom, B. 1963. Some topics in the theory of fluids. *J. Chem. Phys.* 39:2809-2812.
- [35] Sidel, V.W., A.K. Solomon. 1957. Entrance of water into human red cells under an osmotic pressure gradient. *J. Gen. Physiol.* 41:243-257.
- [36] Murata, K., K. Mitsuoka, T. Hirai, T. Walz, P. Agre, J. Heymann, A. Engel, Y. Fujiyoshi. 2000. Structural determinants of water permeation through aquaporin-1. *Nature* 407:599-605.
- [37] Schirmer, Y. 1998. General and specific porins from bacterial outer membranes. *J. Struct. Biol.* 121:101-109.
- [38] Suenaga, A., Komeiji, M. Uebayasi, T. Meguro, M. Saito, I. Yamato. 1998. Computational observation of an ion permeation through a channel protein. *Biosci. Rep.* 18:39-48.
- [39] Tieleman, D.P., H.J.C. Berendsen. 1998. A molecular dynamics study of the pores formed by *E. coli* OmpF porin in a fully hydrated POPE bilayer. *Biophys. J.* 74:2788-2801.

- [40] Schirmer, T., P.Phale. 1999. Brownian dynamics simulation of ion flow through porin channels. *J.Mol.Biol.* 294:1159-1168
- [41] Phale, P., A.Phillipsen, C.Widmer, V.P.Phale, J.P.Rosenbusch, T.Schirmer. 2001. Role of charged residues at the OmpF porin channel constriction probed by mutagenesis and simulation. *Biochemistry* 40:6319-6325.
- [42] Im, W., B.Roux. 2000. A grand canonical Monte Carlo - Brownian dynamics algorithm for simulating ion channels. *Biophys.J.* 79:788-801.
- [43] Roux, B. 2002. Computational studies of the gramicidin channel. *Acc. Chem. Res.* 6:366-375.
- [44] Rostovtseva, T.K., V.M. Aguilera, I. Vodyanoy, S.M. Bezrukov, V.A. Parsegian. 1998. Membrane surface-charge titration probed by gramicidin A channel conductance. *Biophys. J.* 78:1783-1792.
- [45] Busath, D.D., C.D. Thulin, R.W. Hendershot, L.R. Phillips, P. Maughan, C.D. Cole, N.C. Bingham, S. Morrison, L.C. Baird, R.J. Hendershot, M. Cotten, T.A. Cross. 1998. Non-contact dipole effects on channel permeation. I. Experiments with (5F-indole) Trp13 gramicidin A channels. *Biophys. J.* 75:2830-2844.
- [46] Cardenas, A.E., R.D. Coalson, M.G. Kurnikova. 2000. Three-dimensional Poisson-Nernst-Planck theory studies: influence of membrane electrostatics on gramicidin A channel conductance. *Biophys. J.* 79:80-93.
- [47] Agmon, M. 1995. The Grotthuss mechanism. *Chem. Phys. Lett.* 244:456-462.
- [48] Pomes, R., B.Roux. 1998. Free energy profiles for  $H^+$  conduction along hydrogen-bonded chains of water molecules. *Biophys.J.* 75:33-40.
- [49] Pomes, R., B. Roux. 2002. Molecular mechanism of  $H^+$  conduction in the single-file water chain of the gramicidin channel. *Biophys. J.* 82:2304-2316.
- [50] Shrivastava, I.H., D.P Tieleman, P.C.Biggin, M.S.P.Sansom. 2002  $K^+$  versus  $Na^+$  ions in a K channel selectivity filter : a simulation study. *Biophys.J.* 83:633-645.
- [51] Corry, B., T.W.Allen, S.Kuyucak, S.-H. Chung. 2001. Mechanism of permeation and selectivity in calcium channels. *Biophys.J.* 80:195-214.
- [52] Jensen, M., E. Tajkhorshid, K. Schulten. 2001. The mechanism of glycerol conduction in aquaglyceroporin. *Structure* 9:1083-1093.
- [53] de Groot, B.L., H. Grubmüller. 2001. Water permeation across biological membranes : mechanism and dynamics of aquaporin-1 and GlpF. *Science* 294:2353-2357.
- [54] Zhu, F., E. Tajkhorshid, K.Schulten. 2001. Molecular dynamics study of aquaporin-1 water channel in a lipid bilayer. *FEBS Lett.* 504:212-218.
- [55] Tajkhorshid, E., P.Nollert, M.Jensen, L.Miercke, J.O'Connell, R.Stroud, K.Schulten. 2002. Control of the selectivity of the aquaporin water channel family by global orientational tuning. *Science* 296:525-530.
- [56] Cuello, L.G., J.G. Romero, D.M. Cortes, and E. Perozo. 1998. pH-dependent Gating in the *Streptomyces lividans*  $K^+$  channel. *Biochemistry* 37:3229-3236.
- [57] Perozo, E., D.M. Cortes, and L.G. Cuello. 1999. Structural rearrangements underlying  $K^+$ -channel activation gating. *Science* 285:73-78.
- [58] Cortes, D.M., L. G. Cuello, and E. Perozo. 1997. Molecular architecture of full-length KcsA : Role of cytoplasmic domains in ion permeation and activation gating. *J. Gen. Physiol.* 117:165-180.
- [59] Liu, Y.-S., P.Sompornpisut, E.Perozo. 2001. Structure of the KcsA channel intracellular gate in the open state. *Nature Struct. Biol.* 8:883-887.
- [60] Gwan, J.-F., A.Baumgaertner. 2003. Computer simulations of the KcsA gating mechanism. (preprint)
- [61] Sukharov, S., M. Betanzos, C.-S. Chiang, H.R.Guy. 2001. Gating mechanism of the large mechanosensitive channel MscL *Nature* 409:720-724.
- [62] Betanzos, M., C.-S. Chiang, H.R.Guy, S.Sukharev. 2002. A large iris-like expansion of a mechanosensitive channel protein induced by membrane tension. *Nature Struct. Biol.* 9:704-710.
- [63] Perozo, E., A. Kloda, D.Cortes, B. Martinac. 2002. Physical principles underlying the transduction of bilayer deformation forces during mechanosensitive channel gating *Nature Struct. Biol.* 9:696-703.
- [64] Perozo, E., D.Cortes, P.Sompornpisut, A. Kloda, B. Martinac. 2002. Open channel structure of MscL and the gating mechanism of mechanosensitive channels. *Nature* 418:940-948.
- [65] Gullingsrud, J., D.Kosztin, K.Schulten. 2001. Structural determination of MscL gating studied by MD simulations. *Biophys. J.* 80:2074-

- 2081.
- [66] Elmore, D.E., D.A. Dougherty. 2001. Molecular dynamics simulations of wild-type and mutant forms of the *Mycobacterium tuberculosis* MscL channel. *Biophys. J.* 81:1345-1359.
  - [67] Haupts, U., J. Tittor, and D. Oesterheldt. 1999. *Ann. Rev. Biophys. Biomol. Struct.* 28:367-399.
  - [68] Heberle, J. 2000. Proton transfer reactions across bacteriorhodopsin and along the membrane. *Biophys. Biochim. Acta*, 1458:135-147.
  - [69] Lanyi, J. K. 2001. X-Ray Crystallography of Bacteriorhodopsin and Its Photointermediates: Insights into the Mechanism of Proton Transport. *Biochemistry (Moscow)* 66:1192-1196.
  - [70] Edholm, O. O. Berger, F. Jähnig. 1995. Structure and fluctuations of bacteriorhodopsin in the purple membrane : a molecular dynamics study. *J. Mol. Biol.* 250:94-111.
  - [71] Xu, D., M. Sheves, K. Schulten. 1995. Molecular dynamics study of the M412 intermediate of bacteriorhodopsin. *Biophys. J.* 69:2745-2760.
  - [72] Logunov, I., W. Humphrey, K. Schulten, and M. Sheves. 1995. Molecular dynamics study of the 13-cis form (bR<sub>548</sub>) of bacteriorhodopsin and its photocycle. *Biophys. J.* 68:1270-1282.
  - [73] Roux, B., M. Nina, R. Pomes, J. C. Smith. 1996. Thermodynamic stability of water molecules in the bacteriorhodopsin proton channel : a molecular dynamics free energy perturbation study. *Biophys. J.* 71:670-681.
  - [74] Baudry, J., E. Tajkhorshid, F. Molnar, J. Phillips, and K. Schulten. 2001. Molecular Dynamics Study of Bacteriorhodopsin and the Purple Membrane. *J. Phys. Chem. B* 105:905-918.
  - [75] Sass, H.J., Büldt, G. Gessenich, R., Hehn, D., Neff, D., Schlesinger, R., Berendzen, J., Ormos, P. 2000. Structural alterations for proton translocation in the M state of wild-type bacteriorhodopsin. *Nature* 406:649-653.
  - [76] Subramaniam, S., and R. Henderson. 2000. Molecular mechanism of vectorial proton translocation by bacteriorhodopsin. *Nature* 406:653-657.
  - [77] Papadopoulos, G., N. A. Dencher, G. Zaccai, and G. Büldt. 1990. Water molecules and exchangeable hydrogen ions at the active center of bacteriorhodopsin localized by neutron diffraction. *J. Mol. Biol.* 214:15-19.
  - [78] Luecke, H. 2000. Atomic resolution structures of bacteriorhodopsin photocycle intermediates : the role of discrete water molecules in the function of this light-driven ion pump. *Biochim. Biophys. Acta* 1460:133-156.
  - [79] Zaccai, G. 2000. Moist and soft, dry and stiff: a review of neutron experiments on hydration-dynamics activity relations in the purple membrane of *Halobacterium salinarum*. *Biophys. Chem.* 86:249-257.
  - [80] Gottschalk, M., N. A. Dencher, and B. Halle. 2001. Microsecond Exchange of Internal Water Molecules in Bacteriorhodopsin . *J. Mol. Biol.* 311:605-621.
  - [81] Grudinin, S., G. Büldt, and A. Baumgaertner. 2002 Water molecules and hydrogen-bonded networks in bacteriorhodopsin - molecular dynamics study. (preprint 2002)
  - [82] Knapp, E.W., K. Schulten, and Z. Schulten. 1980. Proton conduction in linear hydrogen-bonded systems. *Chem. Phys.* 46:215-229.
  - [83] Tuckerman, M., K. Laasonen, M. Sprik, and M. Parrinello. 1995. Ab initio molecular dynamics simulation of the solvation and transport of H<sub>3</sub>O<sup>+</sup> and OH<sup>-</sup> ions in water. *J. Phys. Chem.* 99:5749-5752.
  - [84] Schmitt, U.W., and G.A. Voth. 1999. The computer simulation of proton transport in water. *J. Chem. Phys.* 111:9361-9381.
  - [85] Marx, D., M.E. Tuckerman, J. Hutter, and M. Parrinello. 1999. The nature of the hydrated excess proton in water. *Nature* 397:601-604.
  - [86] Sagnella, D. E., K. Laasonen, and M. L. Klein. 1996. Ab initio molecular dynamics study of proton transfer in a polyglycine analog of the ion channel gramicidin A. *Biophys. J.* 71:1172-1178.
  - [87] Pomes, R., and B. Roux. 2002. Molecular mechanism of H<sup>+</sup> conduction in the single-file water chain of the Gramicidin channel. *Biophys. J.* 82:2304-2316.
  - [88] Butt, H.J., K. Fendler, E. Bamberg, J. Tittor, and D. Oesterheldt. 1989. Aspartic acids 96 and 85 play a central role in the function of bacteriorhodopsin as a proton pump. *EMBO J.* 8:1557-1663.
  - [89] Zscherp, C., R. Schlesinger, J. Tittor, D. Oesterheldt, and J. Heberle. 1999. *In situ* determination of transient pK<sub>a</sub> changes of internal amino acids of bacteriorhodopsin by using time-resolved attenuated total reflection Fourier-transform infrared spectroscopy. *Proc. Natl. Acad. Sci. USA* 96:5498-5503.
  - [90] Eigen, M. 1964. Proton transfer, acid-base catalysis, and enzymatic hydrolysis. *Ang. Chem. Intern. Ed.* 3:1-72.
  - [91] Meiboom, S. 1961. Nuclear magnetic resonance

- study of the proton transfer in water. *J. Chem. Phys.* 34:375-388.
- [92] Lin, J.H., N.A. Baker, J.A. McCammon. 2002. Bridging implicit and explicit solvent approaches for membrane electrostatics. *Biophys. J.* 83:1374-1379.
- [93] Grudinin, S., M. Zuvic-Butorac, G. Büldt, and A. Baumgaertner. 2003 Distribution of water and hydrogen-bonded networks in the M state of bacteriorhodopsin - a molecular dynamics study. (preprint)
- [94] DaCosta, C.J., Ogrel A.A., McCardy E.A., Blanton M.P., and Baenziger J.E. 2002 Lipid-protein interactions at the nicotinic acetylcholine receptor: a functional coupling between nicotinic receptors and phosphatidic acid-containing lipid bilayers. *J. Biol. Chem.* 277:201-208.
- [95] DeKruijff, B. 1997. Lipids beyond bilayer. *Nature* 386:129-130.
- [96] Van der Does, C., W. van Klompenburg, A. Driessen. 2000. Non-bilayer lipids stimulate the activity of the reconstituted bacterial protein translocase. *J. Biol. Chem.* 275:2472-2478.
- [97] Jentsch, T.J. 2002. Neuronal KCNQ potassium channels : physiology and role in disease. *Nature Rev. Neurosci.* 1:21-30.
- [98] Biggin, P.C., Roosild, T., Choe, S. 2000. Potassium channel structure: domain by domain. *Curr. Opin. Struct. Biol.* 10:456-461.
- [99] Bixby, K.A., Nanao, M.H., Shen, N.V., Kreusch, A., Bellamy, H., Pfaffinger P.J., Choe, S. 1999.  $Zn^{2+}$ -binding and molecular determinants of tetramerization in voltage-gated  $K^+$  channels. *Nature Struct. Biol.* 6:38-43.
- [100] Miyazawa, A., Fujiyoshi, Y., Stowell, M. and Unwin, N. 1999. Nicotinic acetylcholine receptor at 4.6 angstrom resolution: transverse tunnels in the channel wall. *J. Mol. Biol.* 288:765-786.